JCTC Journal of Chemical Theory and Computation

Article

pubs.acs.org/JCTC

Catalytic Role of Dinuclear σ,π-Acetylide Gold(I) Complexes in the Hydroamination of Terminal Alkynes: Theoretical Insights

Gloria Mazzone,[†] Nino Russo,[†,‡] and Emilia Sicilia*[,†]

[†]Dipartimento di Chimica e Tecnologie Chimiche, Università della Calabria, I-87036 Arcavacata di Rende, Italy

[‡]Division de Ciencias Basicas e Ingenieria, Departamento de Quimica, Universidad Autonoma Metropolitana-Iztapalapa, Av. San Rafael Atlixco No. 186, Col. Vicentina, CP 09340 Mexico

Supporting Information

ABSTRACT: A detailed density functional theory (DFT) investigation of the hydroamination of 1-octyne with aniline mediated by a σ,π-digold(I) bulky phosphine-based complex was undertaken in order to shed light on the mechanistic aspects of such processes. With the purpose to probe whether the performance that the cationic digold complexes exhibit is superior to those of mononuclear complexes, the same hydroamination reaction was explored by considering separately the reaction of aniline with both the monogold(I) complexes formed by π- and σ-coordination of 1-octyne to the dialkylbiarylphosphine Au(I) precatalyst. The outcomes of the computational analysis presented here show that, when the σ,π-digold alkynide complex can be formed, the reaction is not necessarily assisted by such a complex, as the computed energy barrier is almost equal to that found when the π-coordinated alkyne mononuclear gold complex is involved in the hydroamination process. The catalytic assistance of the Au(I)−σ-alkynyl complex, instead, can be surely excluded as the hydroamination product is formed by overcoming an energy barrier significantly higher than that computed when both σ,π-digold and π-coordinated alkyne monogold complexes assist the reaction. Moreover, regardless of the implicated gold(I) species, the investigated mechanism accounts for the Markovnikov selectivity of the reaction, confirming the experimental evidence. The proposed mechanisms for the conversion of Au(I) π-coordinated alkyne complexes into the corresponding σ,π-digold alkynide complexes were also explored.

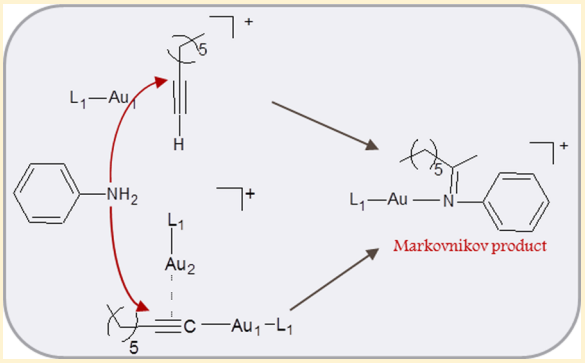

1. INTRODUCTION

The catalysis of organic reactions by gold catalysts has received in the past only little attention because of the preconceived opinion that gold is expensive and inert. The "catalytic gold rush" started with the discovery of the unexpected and quite novel catalytic activity of apparently inert gold in both heterogeneous and homogeneous systems.[1−9]

In the last years, the benefits of gold as a homogeneous catalyst for the synthesis of fine chemicals have emerged in a spectacular fashion.[10−17] The major virtue of gold compounds in homogeneous catalysis is their unique ability to activate C−C multiple bonds as soft, carbophilic Lewis acids, allowing for the formation of new C−C, C−O, C−N, and C−S bonds by nucleophilic attack at these activated substrates.[8,11,13,14,18−21] It is well accepted that the coordination of a C−C multiple bond molecule to a cationic Au(I) complex represents the prototypical mechanistic starting point for Au(I)-catalyzed reactions. Theoretical studies of such π-coordination[22−27] demonstrate that the Au(I) cation cannot significantly participate in Dewar−Chatt−Duncanson-type bonding as antibonding orbitals are too high in energy for significant back-bonding to occur. The lack of back-bonding from Au(I) enhances the electrophilicity of the ligand and favors the attack of the nucleophile.

Acetylene and terminal alkynes, both of which bear a hydrogen atom at one end of the C−C triple bond, can exhibit a second mode of interaction with Au(I) complexes. The terminal hydrogen, due to its acidity, can be replaced by gold in the presence of a base with formation of stable and isolable Au(I)−alkynyl complexes.[28,29] Since the depletion of π-electron density from the alkyne upon coordination to the electrophilic gold(I) center should also enhance the acidity of the terminal proton, alkynyl complexes formation is facilitated. Therefore, under proper reaction conditions dinuclear gold alkynide complexes, showing both π-coordination and gold−alkynyl σ-bond structural motifs, can be formed.[30] Both the Widenhoefer[31] and Corma[32] groups reported the dual σ,π-activation of alkynes and the synthesis of dinuclear gold species. The Widenhoefer group focused the attention on the synthesis and stability of σ,π-digold alkynide complexes,[31] whereas the Corma group explored their importance as intermediates in catalytic transformations.[32] Despite the work of the Corma group, which

Received: September 22, 2014

DOI: 10.1021/ct500849m
J. Chem. Theory Comput. XXXX, XXX, XXX−XXX

Scheme 1

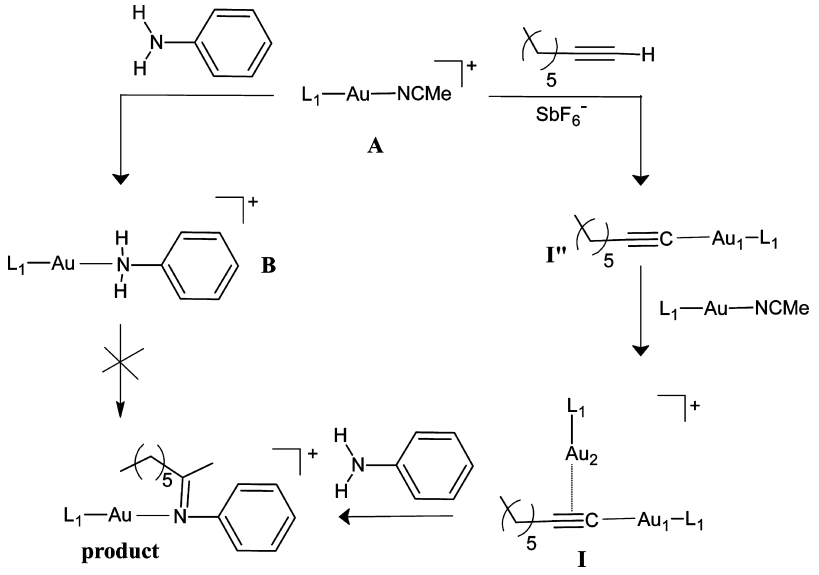

demonstrated that σ,π-digold acetylide species can be active intermediates in catalysis, the role they should play is still matter of debate.[33]

In order to get more information on the role that digold(I)−alkynide complexes can play in catalysis, Corma and co-workers selected the Au(I)-catalyzed hydroamination reaction of terminal alkynes aiming at isolating the active species involved in the catalytic process.[34] The investigation of the intermolecular hydroamination of 1-octyne with aniline carried out by using as precatalyst a gold(I) complex (**A**) bearing a bulky dialkylbiarylphosphine ligand showed that the corresponding σ,π-digold alkynide complex is formed and cationic digold complexes as intermediates are formed in prevalence. The influence of the nature of the terminal alkyne and the bulkiness of the Au(I) ligand on the stability of the digold complexes was also explored. Two independent experiments were carried out by mixing, in the beginning, the dialkylbiarylphosphine Au(I) complex **A** with either 1-octyne or aniline and, on the basis of the results of X-ray, NMR, and MALDI-TOF-MS analyses, a hypothesis on the structures of the intermediates formed before the release of the final products was formulated as shown in Scheme 1. It was also reported that only the Markovnikov product is formed.

Inspired by such experiments, we have investigated, with the aid of density functional theory (DFT) calculations, the detailed mechanism of the whole hydroamination of 1-octyne with aniline reaction implicating the **I** complex according to the proposal summarized in Scheme 1.

Moreover, aiming at answering to the question whether in gold catalysis two centers are better than one,[35] the same hydroamination reaction was studied by considering separately the reaction of aniline with both the monogold(I) complexes formed by π- and σ-coordination **I′** and **I″**, respectively of 1-octyne to the precatalyst (**A**).

The envisaged mechanisms able to account for the conversion of Au(I) π-coordinated alkyne complexes into the corresponding σ,π-digold alkynide complexes were also explored according to the proposals in Scheme 2.

The mechanisms of gold catalyzed reactions under homogeneous conditions are rather complex and the isolation of key intermediates is challenging. Therefore, as previously

Scheme 2

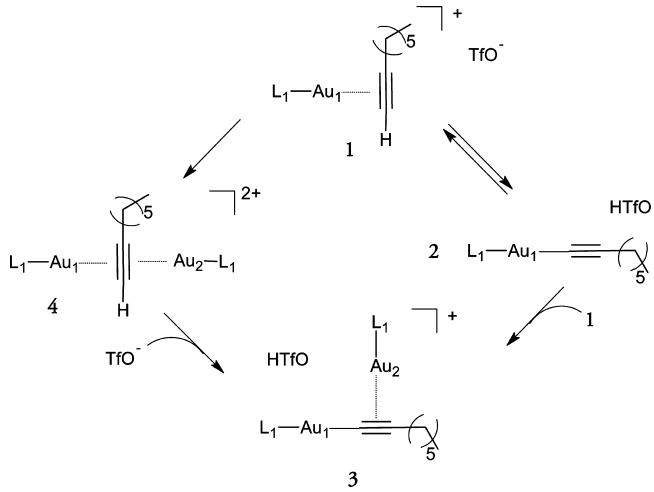

well underscored,[36] a mechanistic understanding was often based on analogy and speculation. DFT calculations, along with labeling and kinetic experiments, significantly contributed to the advancement of coherent mechanistic schemes. The theoretical analysis reported in this work is expected to be helpful in elucidating whether, once formation of σ,π-digold alkynide complexes is accessible, their assistance in gold-catalyzed reactions can result to be advantageous.

2. COMPUTATIONAL DETAILS

Numerous theoretical studies of Au-catalyzed reactions at the B3LYP[37,38] level have been reported in the literature, which confirm that such functional is quite suitable to investigate Au-catalyzed reactions.[22,39−43] Nevertheless, a survey of the recent literature shows that some benchmark studies on gold complexes devoted to the evaluation of the accuracy of different DFT exchange-correlation functionals were carried out.[44−50] From such investigations it results that the best performance can be obtained by employing the very computationally expensive double hybrid B2PLYP functional. Other well-performing functionals were selected to obtain quite

DOI: 10.1021/ct500849m
J. Chem. Theory Comput. XXXX, XXX, XXX−XXX

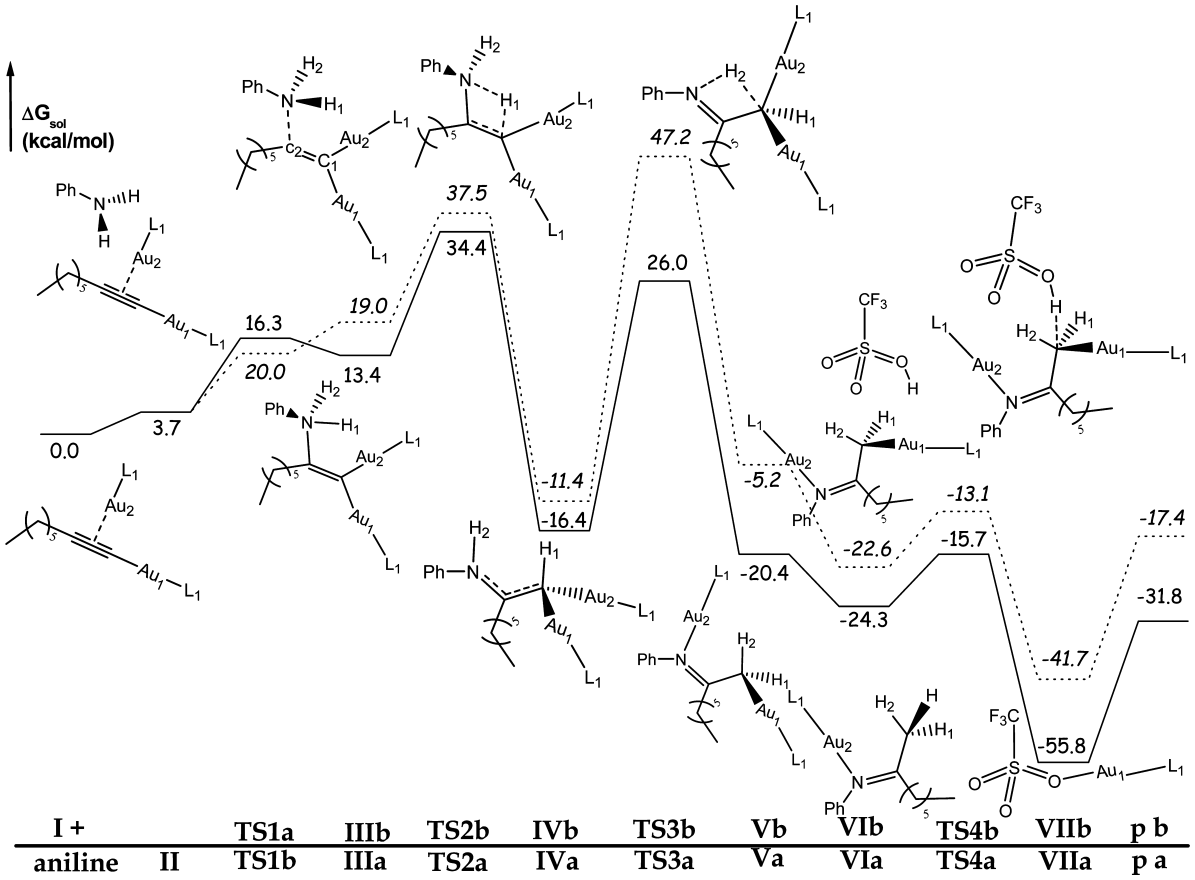

Figure 1. Calculated B3LYP-D3 free energy profiles for the reaction of the σ,π-digold alkynide complex **I** with aniline. The formation of both Markovnikov (solid line) and anti-Markovnikov (dashed line) products is reported. All the species depicted in this figure are charged +1. Relative Gibbs free energies at 298.15 K in dichloromethane solvent are in kilocalories per mole.

accurate results. Due to both the size of the systems under investigation and the huge number of stationary points located along the explored reaction pathways, in the present paper, the use of very computationally costly functionals was ruled out. Moreover, lacking any experimental information on the energetics, the main aim of the work was the comparison at the same level of theory of the catalytic performance of mono- and digold complexes. Therefore, density functional theory calculations were performed employing the B3LYP exchange-correlation functional as implemented in the Gaussian09 package.[51] To restrain the computational effort required by the rigorous search of all the minima and transition state involved by mechanistic proposals in Scheme 1 and 2 as well as along the pathways for monogold complexes, the biphenyl and *t*Bu groups of the real bulky biphenyl-based phosphine ligand were preliminarily replaced with less demanding phenyl and methyl groups, respectively. All the intercepted minima and transition states were reoptimized by using the real biphenyl groups, whose presence showed to influence the energetics of the reaction steps due to the weak interactions they can establish with Au atoms and including dispersion corrections in the B3LYP functional following Grimme's approach (B3LYP-D3).[52] Methyl groups, instead, were not replaced by bulky *t*Bu, since the energetics does not change appreciably. For Au, the relativistic compact Stuttgart/Dresden effective core potential[53] was used in conjunction with its split valence basis set. Standard 6-31G basis set of Pople for carbon and hydrogen atoms of phenyl rings and methyl groups on P was used together with the 6-31G** for the rest of the atoms, except O and S atom of triflic acid, for which a diffuse function was added. Such a level of theory will be indicated as BS1. To check the influence of the basis set size, the structure of the σ,π-digold alkynide complex **I** was fully optimized by using more extended basis sets on all atoms, that is standard 6-311G* basis set on carbon and hydrogen atoms of phenyl rings and methyl groups on P together with the 6-311+G** for the rest of the atoms (BS2). Final energies were evaluated by performing single-point calculations on the optimized geometries employing the B3LYP-D3 functional together the 6-311++G** standard basis set for all the atoms except Au.

All of the reported structures represent genuine minima or transition states on the respective potential energy surfaces, as confirmed by analysis of the corresponding Hessian matrices. Intercepted transition states were checked by IRC (intrinsic reaction coordinate) analysis.[54,55] The impact of solvation effects on the energy profiles was estimated by using the self-consistent-reaction-field polarizable continuum model (PCM)[56] as implemented in Gaussian 09. The UFF set of radii has been used to build up the cavity. Since preliminary calculations have clearly shown geometry relaxation effects to be not significant, the solvation Gibbs free energies were calculated in implicit dichloromethane (ε = 8.93), the solvent medium in the experiments, with the B3LYP-D3 functional and triple-ζ quality basis sets as illustrated above by performing single-point calculations on all stationary points structures obtained from vacuum calculations.

Reaction Gibbs free energies in solution, ΔG_{sol}, were calculated for each process as the sum of two contributions: a

DOI: 10.1021/ct500849m
J. Chem. Theory Comput. XXXX, XXX, XXX−XXX

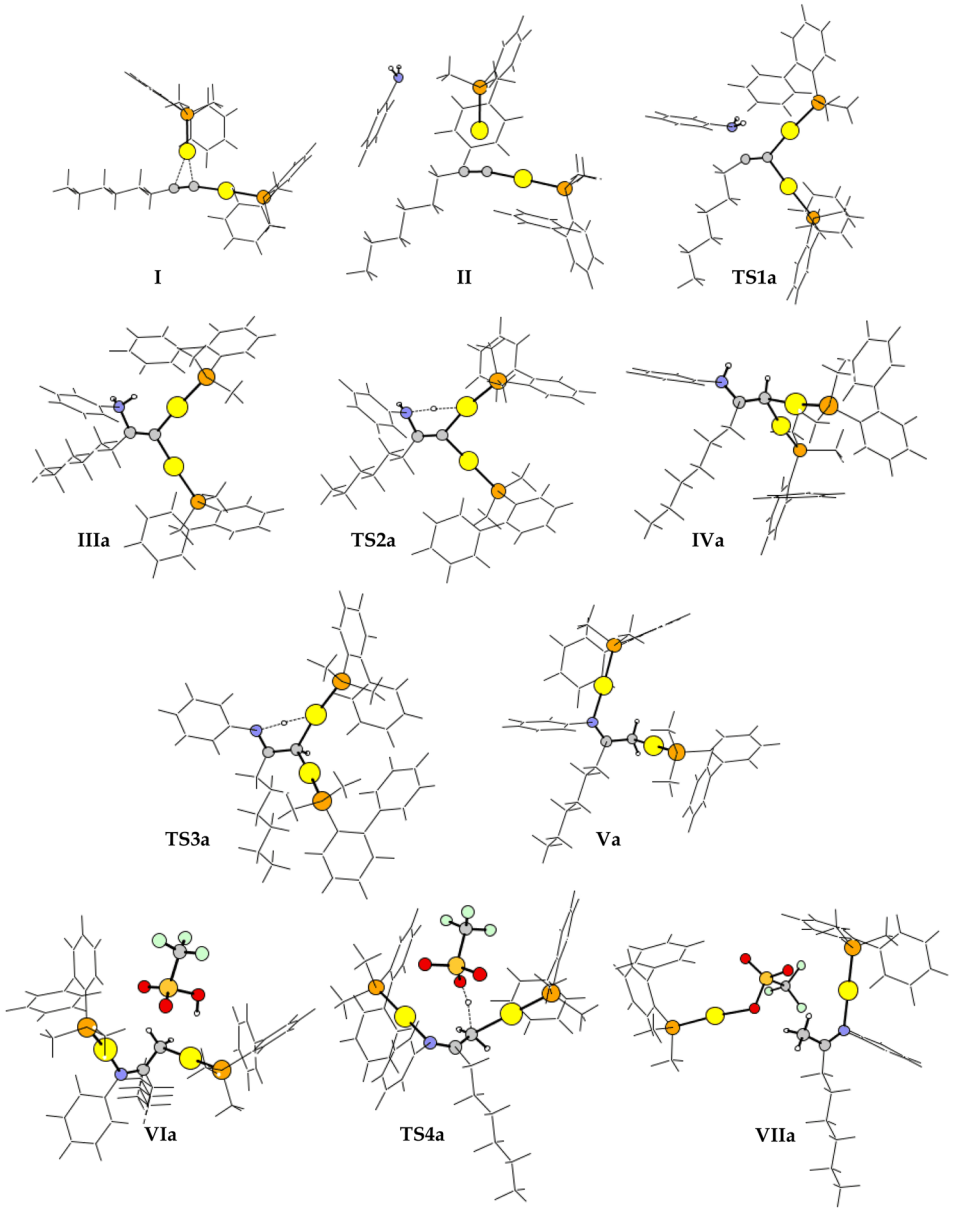

Figure 2. B3LYP-D3 fully optimized structures of stationary points computed along the Markovnikov product formation pathway starting from the σ,π-digold alkynide complex **I** and aniline.

gas-phase reaction free energy, ΔG_{gas}, and a solvation reaction free energy term calculated with the continuum approach, ΔG_{solv}. Nevertheless, such an approach does not reflect the real entropic cost under catalytic conditions, and the effects are particularly relevant when substrate association and dissociation are taken into consideration.[57] Following a common approach in theoretical catalysis, the solvation entropy has been estimated as two/third of its gas-phase value.[57,58]

3. RESULTS AND DISCUSSION

3.1. Hydroamination of 1-Octyne with Aniline Implicating a σ,π-Digold Alkynide Complex. As anticipated above, when independent experiments were carried out mixing Au(I) complex **A** with either 1-octyne or aniline, formation in good yields of both corresponding digold complex **I** and Au(I)-amine complex **B** was observed. The possibility that the title reaction starts with the amine activation by the precatalyst was explored, but with very high calculated energy barriers, this reaction channel was ruled out (see S1 of the Supporting Information for details).

A detailed description of the catalytic mechanism of the hydroamination process promoted by such a complex is presented here, whereas the outcomes of the exploration of the formation mechanism of the σ,π-digold alkynide complex will be discussed later.

Calculated energy profiles for the reaction of the σ,π-digold alkynide complex with aniline are shown in Figure 1. Both Markovnikov and anti-Markovnikov products formation was examined. Structures of reactants, intermediates, transition states, and products of the reaction leading to the Markovikov product are schematically depicted in the same figure. Fully optimized B3LYP-D3 structures intercepted along the Markovnikov product formation are sketched in Figure 2, while those located along the anti-Markovnikov pathway are reported in Figure S2 of the Supporting Information. As reported in Table S3 of the Supporting Information, the good

DOI: 10.1021/ct500849m
J. Chem. Theory Comput. XXXX, XXX, XXX−XXX

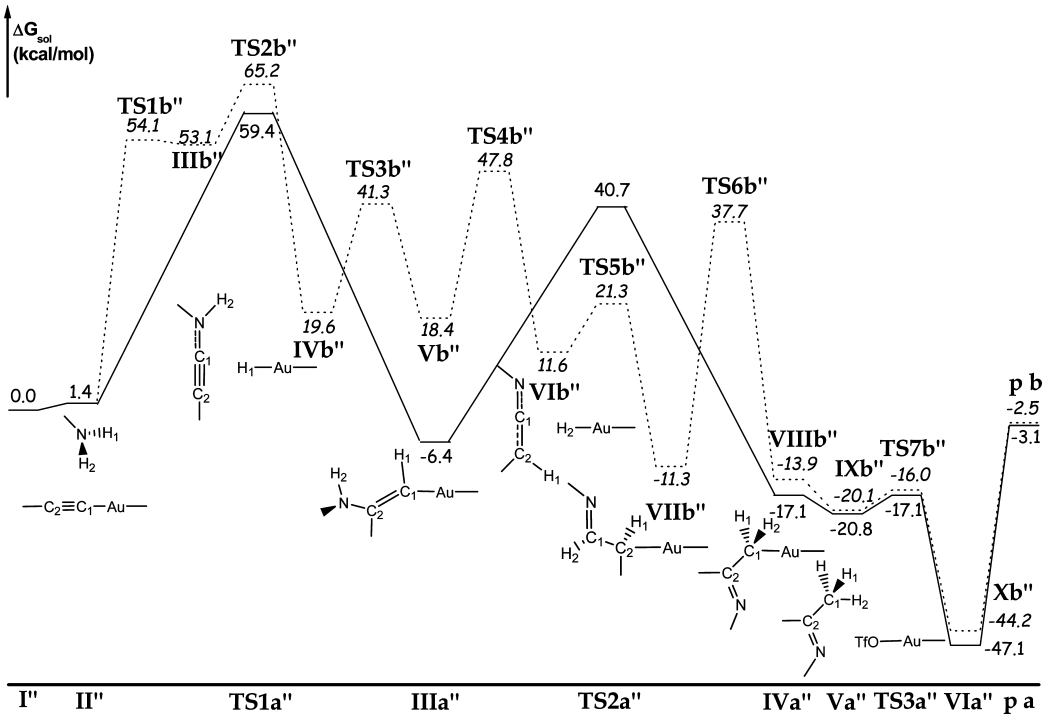

Figure 3. Calculated B3LYP-D3 free energy profiles for the reaction between octyne and aniline assisted by the $[Au{-}P((Me)_2(BPh))]^+$ complex. Both Markovnikov (solid line) and anti-Markovnikov (dashed line) products formation is reported. All the species depicted in figure are charged +1. Relative Gibbs free energies at 298.15 K in dichloromethane solvent are in kilocalories per mole.

agreement between the ground-state optimized geometrical parameters and the most relevant available experimental structural features[34] of the reference complex **I** indicates a good modeling of the catalysts. The only exception is represented by the length of the C1−C2 triple bond, whose measured experimental value seems to be too short. Moreover, the adoption of more extended basis sets does not cause significant changes.

Unless otherwise noted, in what follows, the discussed energies are B3LYP-D3 relative Gibbs free energies at 298 K in dichlorometane (ΔG_{sol}) calculated with respect to the digold complex, named **I**, and aniline reactants reference energy. The cationic digold complex is characterized by both σ to Au1 and π to Au2 coordination of octyne, at 2.033 and 2.220 Å distances, respectively from the C1 atom.

From the energy profile in Figure 1 it is evident that, once the σ,π-digold alkynide complex is formed, the first step along the intermolecular hydroamination pathway involves a preliminary interaction between the reactants, to form intermediate **II**, which requires 3.7 kcal/mol to occur. In such intermediate the aniline weakly interacts with the σ,π-digold alkynide complex, as no significant structural change is observed. From the intermediate **II** the reaction can proceed following either Markovnikov or anti-Markovnikov attack of aniline to the triple bond. Thus, the attack of aniline on the C2 atom provides the Markovnikov product (pathway a, solid line in Figure 1). When the C1 atom undergoes the attack, the anti-Markovnikov product (pathway b, dotted line in Figure 1) is formed. Along the Markovnikov pathway we have intercepted a transition state for the attack of aniline to the C2 atom, **TS1a**, lying at 16.3 kcal/mol above the reference energy, in which the aniline approaches the C2 atom from the opposite side in respect to the gold atoms. The attack of aniline causes important changes in the structure of the σ,π-digold alkynide complex since both gold atoms coordinate the C1 one. The intermediate **IIIa** is more stable by 2.9 kcal/mol than the transition state leading to it, although their structures are quite similar.

The subsequent H2 atom shift to form the intermediate **Va** via **TS3a** takes place overcoming an energy barrier of 42.4 kcal/mol with an energy gain of 20.4 kcal/mol. In such intermediate the definitive formation of the N═C double bond (1.316 Å) is observed.

The final step of the reaction, that is formation of the hydroamination Markovnikov product, requires the intervention of an acid able to protonate to the C1 atom. Therefore, by using the triflic acid as protonating agent, a minimum **VIa** in which the acid weakly interacts with the complex **Va** has been intercepted, lying at −29.3 kcal mol^{-1}. The H atom transfer takes place via **TS4a** overcoming an energy barrier of 8.9 kcal/mol. In the final product **VIIa**, which is stabilized by 55.8 kcal/mol with respect to the reference energy, coordination of C1 to the Au1 atom is definitively lost, being the coordination site now occupied by the triflate anion. The catalytic cycle could be, then, closed by the release of the Markovnikov product that requires 24.0 kcal/mol to occur. The step that controls the reaction rate of the overall process is clearly the hydrogen shift third step, which involves the highest amount of energy (42.4 kcal/mol) to take place.

Looking at the potential energy surface computed for the formation of the anti-Markovnikov product in Figure 1 (dashed line), it is clear that such formation results energetically unfavorable, by both kinetic and thermodynamic points of view. Indeed, starting from the same intermediate **II**, involved in the process described above, not only all the intercepted minima and transition states lie at higher energy in respect to those describing the Markovnikov product formation, but also the rate-limiting step requires 58.6 kcal/mol to take place.

DOI: 10.1021/ct500849m
J. Chem. Theory Comput. XXXX, XXX, XXX−XXX

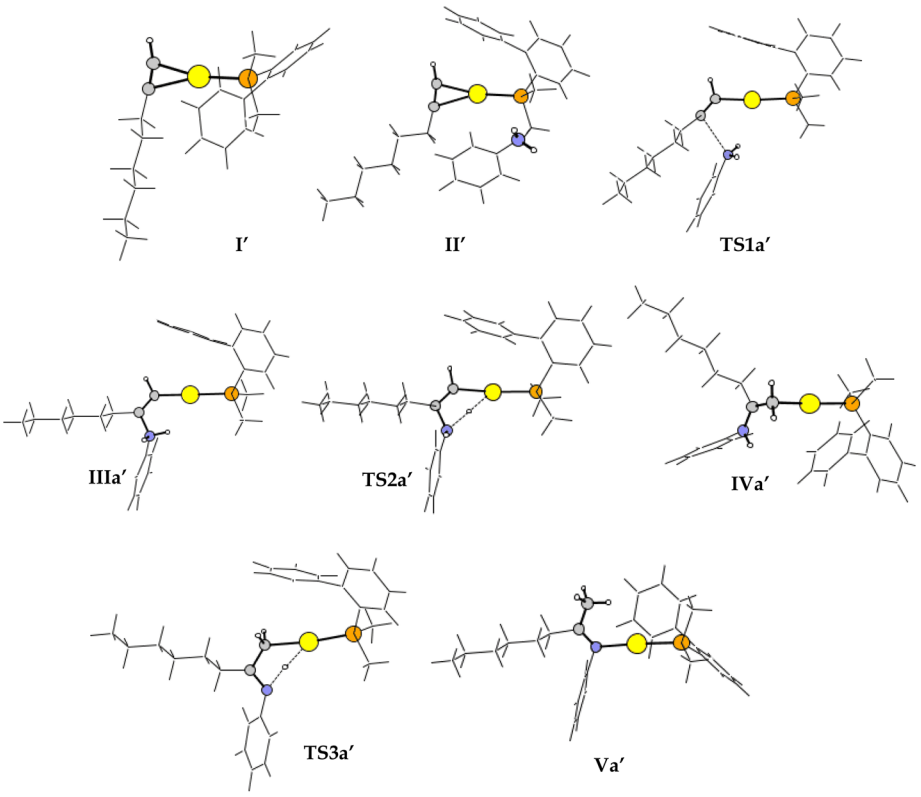

Figure 4. B3LYP-D3 fully optimized structures of stationary points computed along the Markovnikov pathway for the hydroamination of 1-otyne with aniline catalyzed by the gold(I) $[Au{-}P((Me)_2(BPh))]^+$ complex.

3.2. Hydroamination of 1-Octyne with Aniline Assisted by a Au−Alkyne Complex. As the declared purpose of the present paper was to establish whether the performance that the cationic digold complex **I** exhibits can be superior to the mononuclear complexes, the same mechanistic investigation of the hydroamination reaction of 1-octyine with aniline assisted by the corresponding π monogold alkyne complex, labeled $[Au{-}P((Me)_2(BPh))]^+$, was undertaken.

B3LYP-D3 calculated energy profiles are reported in Figure 3. In analogy with the investigation reported above, both Markovnikov and anti-Markovnikov product formation were investigated and all the structures of intercepted stationary points describing the Markovnikov product formation are schematically depicted in the same figure. Fully optimized B3LYP-D3 structures intercepted along such pathways are sketched in Figure 4, while those located along the anti-Markovnikov pathway are reported in Figure S6 of the Supporting Information.

Figure 3 shows that the reaction starts with the primary interaction between gold(I) complex and the alkyne which leads to the intermediate **I′** formation. Such intermediate is characterized by the typical coordination of a multiple bond to the Au(I) center, in which the gold atom lies at 2.234 and 2.437 Å from C1 and C2 atoms, respectively. The precoordination of the aniline in the intermediate **II′** does not introduce significant changes in the coordination mode of the octyne to the gold atom, which remains of π-type.

As can be clearly inferred from the comparison between solid (Markovnikov pathway) and dashed (anti-Markovnikov product) lines in Figure 3, the Markovnikov process is computed to be more favorable with respect to the anti-Markovnikov one. The Markovnikov pathway involves the attack of aniline to the C2 atom, which proceeds with an activation barrier of 8.8 kcal/mol. The formed **IIIa′** complex lies 18.5 kcal/mol lower in energy with respect to the transition state **TS1a′** leading to it.

The reaction continues with the concerted gold-assisted proton transfer from N atom to the C1 one. The rearrangement of **IIIa′** to **IVa′** complex via the transition state, **TS2a′**, requires 26.4 kcal/mol to take place. The formed complex, **IVa′**, lying at 51.2 kcal/mol below the energy of reactants, is much more stable than the intermediate from which it derives. Also the next step, the second hydrogen transfer from nitrogen to the C1 atom, occurs in a concerted manner. IRC calculations performed for both transition state, **TS2a′** and **TS3a′**, confirm that the gold atom assists the H-transfer processes, acting as a proton shuttle, even if no intermediate in which the H atom is directly bonded to the gold one is found. The second transfer requires a higher amount of energy to occur with respect to the first one (42.2 vs 26.4 kcal/mol) and represents the slower step of the whole process. The formed complex **Va′**, in which the Markovnikov product is still coordinated to the metal center through the nitrogen atom, is strongly stabilized as it lies 58.5 kcal/mol below the reference energy. The catalytic cycle that is calculated to be endothermic by 31.0 kcal/mol could be, thus, closed by the product release.

As anticipated before, the activation energy barrier along the reaction pathway leading to formation of the anti-Markovnikov product is higher than that found for the Markovnikov one (66.0 vs 42.2 kcal/mol). Additional structural information about the anti-Markovnikov product can be found in Figure S5 of the Supporting Information.

3.3. Hydroamination Catalytic Process of Au(I)−Alkynyl Complex with Aniline. It has been also considered the possibility that, once the terminal proton of 1-octyne is

DOI: 10.1021/ct500849m
J. Chem. Theory Comput. XXXX, XXX, XXX−XXX

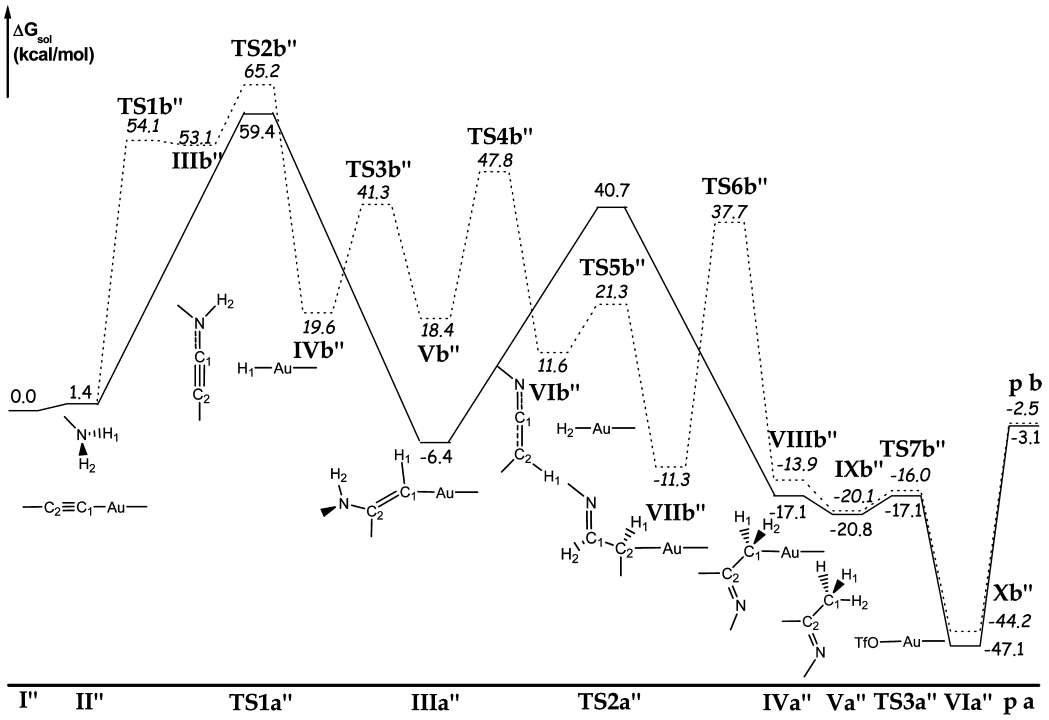

Figure 5. Calculated B3LYP-D3 free energy profiles for the reaction between Au-alkynyl complex **I**″ and aniline. Both Markovnikov (solid line) and anti-Markovnikov (dashed line) products formation is reported. Relative Gibbs free energies at 298.15 K in dichloromethane solvent are in kilocalories per mole.

replaced by gold in the presence of a base, the formed Au(I)-alkynyl complex **I**″ could undergo the attack of the aniline nucleophile before the formation of the *σ,π*-digold alkynide complex.

In Figure 5 are reported the B3LYP-D3 calculated energy profiles for the reaction pathways which lead to both Markovnikov and anti-Markovnikov products and a schematic representation of the intercepted minima along the Markovnikov pathway. In Figure S5 and S6 of the Supporting Information are depicted all the intercepted optimized structures.

The hydroamination process involving the Au(I)−alkynyl complex starts with the interaction between the gold complex **I**″ and the nucleophile which leads to the formation of the adduct **II**″, whose formation requires 1.4 kcal/mol to occur. Following the Markovnikov attack (pathway a, solid line), the aniline approaches the C2 atom from the opposite side with respect to the coordinated catalyst and transfers one of its hydrogens to the C1 atom in a concerted manner, through the **TS1a**″. Such a rearrangement, which requires 58.0 kcal/mol to take place, yields the intermediate **IIIa**″, which lies 6.4 kcal/mol below the reference energy. The reaction proceeds with the second H-transfer from the nitrogen atom to the C1 one, through the **TS2a**″, in order to form the intermediate **IVa**″. Formation of such intermediate, occurs overcoming an energy barrier of 47.1 kcal/mol and without the assistance of the metal center as proton shuttle, since aniline has approached the triple bond from the opposite side in respect to the gold atom. The last step of the reaction yielding the Markovnikov product involves the triflic acid that is responsible of the H-transfer from its oxygen atom to the C1 one, through the transition state **TS3a**″. For the rearrangement, exothermic by 47.1 kcal/mol, that leads to the formation of the most stable intermediate **VIa**″ 3.7 kcal/mol are required. The final release of the product needs 44.0 kcal/mol to occur.

As it appears from a comparison between the reaction profiles for the Markovnikov and the anti-Markovnikov attacks reported in Figure 5, an interesting difference exists, not observed in the pathways described in the previous sections. The anti-Markovnikov pathway (pathway b, dashed line) is described by more steps than those along the Markovnikov hydroamination profile due to the formation of linear complexes, for both **IVb**″ and **VIb**″ intermediates, of the type $[LAu-H]^+$ schematically depicted in figure, the temporary detachment of the substrate from the metal coordination site and subsequent rearrangement. This difference makes the Markovnikov pathway more amenable. Moreover, the energy barriers computed for the first step along both the Markovnikov and anti-Markovnikov attacks are very high compared with the preferred Markovnikov pathways described in the previous sections.

In order to easily compare the energetics of all the investigated processes, the calculated activation barriers for the rate-determining step of each investigated hydroamination process were collected in Table 1.

Table 1. Activation Barriers ($\Delta E^{\#}$; kcal/mol) Calculated for the Rate-Determining Step of the Hydroamination Catalytic Process Involving All the Considered Gold(I) Complexes[a]

	σ,π-digold alkynide complex		Au(I)−alkyne complex		Au(I)−alkynyl complex	
	a	b	a	b	a	b
$\Delta E^{\#}$	42.4	58.6	42.2	66.0	58.0	52.7

[a]The labels a and b indicate the pathway computed for the Markovnikov and anti-Markovnikov product formation, respectively.

DOI: 10.1021/ct500849m
J. Chem. Theory Comput. XXXX, XXX, XXX−XXX

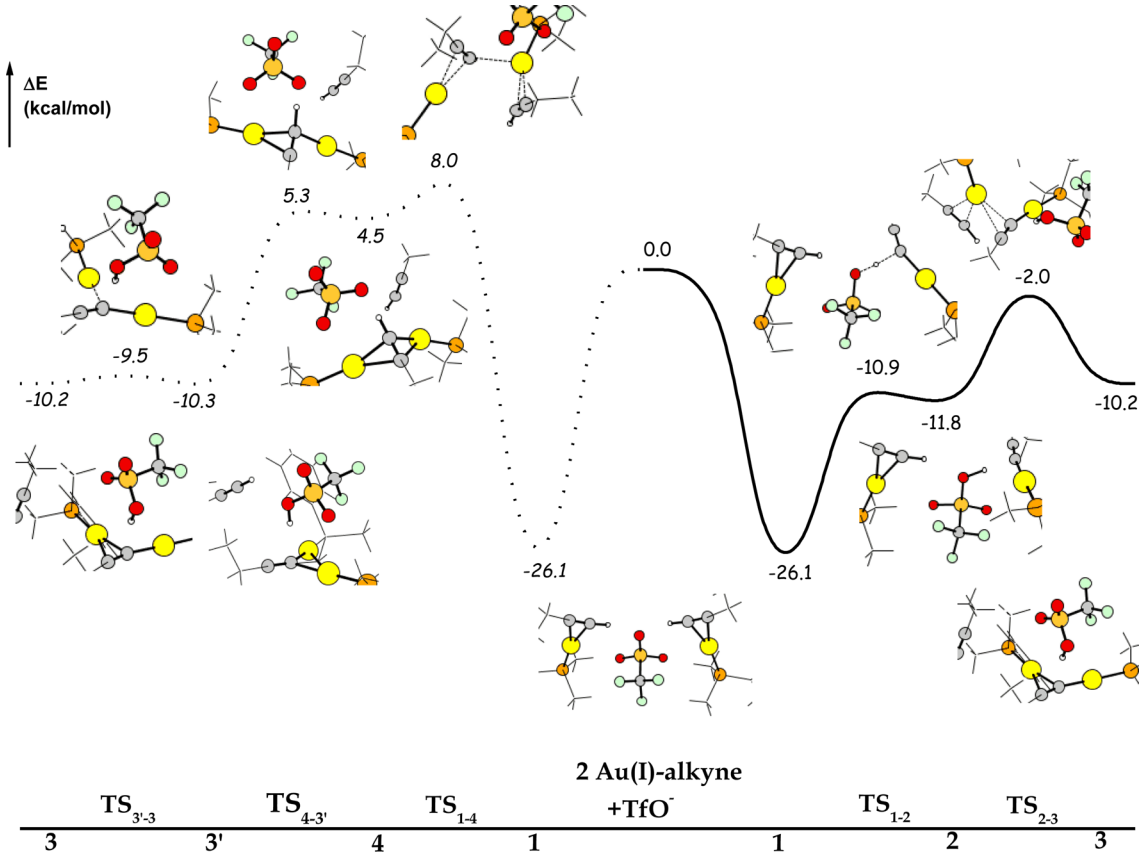

Figure 6. Calculated B3LYP zero-point corrected energy profiles for the conversion of Au−alkyne complex **1** into the σ,π-digold alkynide complex **3** via Au-alkynyl complex **2** (solid line) and via π,π-digold complex **4** (dashed line). Relative energies at 298.15 K are in kilocalories per mole.

According to such data, the Au(I)−alkynyl-assisted reaction pathway is energetically unfavorable with respect to the other ones, as well as the process which accounts for the anti-Markovnikov product formation in which either the σ,π-digold alkynide or the Au(I)−alkyne complexes are involved.

3.4. Formation of Dinuclear σ,π-Alkynide Complex. As reported by both Widenhoefer and Corma groups, the conversion of Au(I) π-coordinated alkyne complexes into the corresponding σ,π-digold alkynide complexes can be easily realized under proper conditions.[7,10] The mechanisms proposed by Widenhoefer for the σ,π-digold alkynide complexes formation (see Scheme 2) have been investigated. In order to keep the computational cost low, both a simplest model of a biphenyl-based phosphine ligated gold(I) complex and a less demanding alkyne were employed. That is, the $[Au-P((Ph)(Me)_2)]^+$ complex and 1-butyne were selected for such calculations. The anion of the triflic acid was chosen to act as the involved base.

According to Scheme 2, the mechanisms by which the σ,π-digold alkynide complex can be formed are essentially two. In the first one a base abstracts the acetylenic proton from the Au(I)−alkyne complex **1**, to form the species **2**, before the coupling of the two gold complexes which leads to the species **3**. The alternative mechanism involves first the formation of a π,π-digold species **4** and then the alkyne deprotonation to yield the digold catalyst **3**.

Figure 6 illustrates the energy profile for the conversion of Au−alkyne complex **1** into the σ,π-digold alkynide complex **3** via Au−alkynyl complex **2** (solid line) and via π,π-digold species **4** (dashed line). In the same figure the most relevant portion of all the optimized structures is reported at each intercepted stationary point. The discussed energies are B3LYP relative zero-point corrected energies calculated with respect to the sum of the two Au(I)-alkyne complex and triflate anion energies.

Looking at Figure 6, regardless of the path followed by the reaction, formation of the first adduct (**1**) is exothermic by 26.1 kcal/mol with respect to separated reactants. In such adducts the triflate anion establishes a weak interaction with both the Au(I)−π-alkyne complexes through their acetylenic protons.

According to the first pathway (solid line), the deprotonation of 1-butyne by TfO^- occurs through the $\mathbf{TS}_{1-2}$ and requires about 15 kcal/mol to take place. In such a transition state the triflate atom abstracts the acetylenic proton from one of the alkyne molecules coordinated to the metal center. The σ-bond between the C1 and Au1 atoms is almost already formed, being the Au−C1 distance and Au−C1−C2 angle 2.045 Å and 155.7°, respectively. The formed intermediate **2** is only slightly more stable than the transition state leading to it, and it is characterized by a weak interaction between the formed triflic acid proton and the triple bond of the alkyne directly bound to the gold atom. In the next step the two Au(I) complexes approach so that the alkyne π-coordinated to the Au2 is released and the σ,π-digold alkynide complex **3** is formed. In the involved transition state, $\mathbf{TS}_{2-3}$, the formed triflic acid does not play any role. Such a rearrangement requires less than 10 kcal/mol to occur.

Following the alternative pathway (dashed line), conversion of the Au−alkyne complex **1** into the σ,π-digold alkynide complex **3** involves, before the deprotonation of one of the

DOI: 10.1021/ct500849m
J. Chem. Theory Comput. XXXX, XXX, XXX−XXX

alkyne molecules, the initial coupling between the gold−π-alkyne complexes. Release of one alkyne and formation of the corresponding intermediate **4** requires more than 34 kcal/mol to take place. The product of such rearrangement lies 30.6 kcal/mol higher in energy than the previous minimum. It is characterized by a π-coordination of the same alkyne to both the gold atoms, which enhances the acidity of the acetylenic proton. Indeed, the subsequent proton abstraction step requires less than 1 kcal/mol to take place forming the intermediate **3′**. Such an intermediate is characterized by a σ-coordination of both Au1 and Au2 atoms to the same carbon atom C1 of the alkyne. Rearrangement of intermediate **3′** to the desired σ,π-digold alkynide complex **3** can occur, through $\mathbf{TS}_{3-3'}$, overcoming a very low energy barrier. From our calculations, it results that the first described mechanism is more favorable and accounts for the conversion of π-alkyne gold complexes into σ,π-digold alkynide complexes.

4. CONCLUSIONS

The investigation of the whole hydroamination process of 1-octyne with aniline catalyzed by gold(I) complexes has been carried out and all the mechanistic hypotheses existing in the literature have been fully explored.

The implication of σ,π-digold alkynide complex in the hydroamination of 1-otyne with aniline, as well as those of the correspondent monogold(I) complexes with alkyne σ- and π-coordinated, respectively, have been elucidated. The possibility that Au(I)−amine complex can participate to the title reaction has been also investigated. Our calculations show that the Au(I)−amine complex cannot further react to achieve the hydroamination product since the reaction requires overcoming a high energy barrier.

Moreover, the investigated mechanism accounts for the Markovnikov selectivity of the reaction, confirming thus the experimental evidence. Indeed, the Markovnikov product requires a lower amount of energy to be formed than the anti-Markovnikov one, when the digold catalyst is considered. Calculations show how, when the σ,π-digold alkynide complex is formed, the reaction is not necessarily assisted by such complex, as the computed energy barrier is almost equal to that found when π-coordinated alkyne mononuclear gold complex is involved in the hydroamination process. The catalytic assistance of the Au(I)−σ-alkynyl complex can be surely excluded as the hydroamination product is formed by overcoming an energy barrier significantly higher.

Conversion of Au(I) π-complexes of alkynes into σ,π-digold alkynide complexes via a Au−alkynyl complex results to be to be most favorable pathway.

The theoretical insights presented in this work are expected to help the understanding of such gold-catalyzed hydroamination reactions as well as similar processes.

■ ASSOCIATED CONTENT

Supporting Information

Details about the investigated reaction starting from Au(I)−aniline complex and 1-octyne; selected structural parameters of complex **I** obtained by using BS1 and BS2 compared with experimental ones; B3LYP-D3 fully optimized structures of stationary points computed along the anti-Markovnikov product formation starting from the σ,π-digold alkynide complex **I** and aniline; B3LYP-D3 fully optimized structures of stationary points computed along the anti-Markovnikov pathway for the hydroamination of 1-otyne with aniline catalyzed by the gold(I) complex **I′**; B3LYP-D3 fully optimized structures of stationary points computed along the Markovnikov pathway for the reaction between Au-alkynyl complex **I″** and aniline; B3LYP-D3 fully optimized structures of stationary points computed along the anti-Markovnikov pathway for the reaction between Au-alkynyl complex **I″** and aniline. This material is available free of charge via the Internet at http://pubs.acs.org.

■ AUTHOR INFORMATION

Corresponding Author

*E-mail: siciliae@unical.it.

Notes

The authors declare no competing financial interest.

■ ACKNOWLEDGMENTS

Università della Calabria and Dipartimento di Chimica e Tecnologie Chimiche are gratefully acknowledged.

■ REFERENCES

(1) Hutchings, G. J. *J. Catal.* **1985**, *96*, 292−295.
(2) Haruta, M.; Kobayashi, T.; Sano, H.; Yamada, N. *Chem. Lett.* **1987**, *16*, 405−408.
(3) Thompson, D. *Gold Bull.* **1998**, *31*, 111−118.
(4) Bond, G. C. *Catal. Today* **2002**, *72*, 5−9.
(5) Teles, J. H.; Brode, S.; Chabanas, M. *Angew. Chem., Int. Ed.* **1998**, *37*, 1415−1418.
(6) Mizushima, E.; Sato, K.; Hayashi, T.; Tanaka, M. *Angew.Chem., Int. Ed.* **2002**, *41*, 4563−4565.
(7) Hashmi, A. S. K. *Chem. Rev.* **2007**, *107*, 3180−3211.
(8) Corma, A.; Leyva-Pérez, A.; Sabater, M. J. *Chem. Rev.* **2011**, *111*, 1657−1712.
(9) Hopkinson, M. N.; Gee, A. D.; Gouverneur, V. *Chem.—Eur. J.* **2011**, *17*, 8248−8262.
(10) Hashmi, A. S. K. *Chem. Rev.* **2007**, *107*, 3180−3211.
(11) Jiménez-Nuñez, E.; Echavarren, A. M. *Chem. Commun.* **2007**, 333−346.
(12) Fürstner, A.; Davies, P. W. *Angew. Chem., Int. Ed.* **2007**, *46*, 3410−3449.
(13) Jiménez-Nuñez, E.; Echavarren, A. M. *Chem. Rev.* **2008**, *108*, 3326−3350.
(14) Gorin, D. J.; Sherry, B. D.; Toste, F. D. *Chem. Rev.* **2008**, *108*, 3351−3378.
(15) Fürstner, A. *Chem. Soc. Rev.* **2009**, *38*, 3208−3221.
(16) Shapiro, N. D.; Toste, F. D. *Synlett* **2010**, 675−691.
(17) Patil, N. T.; Yamamoto, Y. *Chem. Rev.* **2008**, *108*, 3395−3442.
(18) Arcadi, A. *Chem. Rev.* **2008**, *108*, 3266.
(19) Li, Z.; Brouwer, C.; He, C. *Chem. Rev.* **2008**, *108*, 3239.
(20) Michelet, V.; Toullec, P. Y.; Genêt, J.-P. *Angew. Chem., Int. Ed.* **2008**, *47*, 4268.
(21) Amijs, C. H. M.; López-Carrillo, V.; Raducan, M.; Pérez-Galén, P.; Ferrer, C.; Echavarren, A. M. *J. Org. Chem.* **2008**, *73*, 7721.
(22) Mazzone, G.; Russo, N.; Sicilia, E. *J. Chem. Theory Comput.* **2010**, *6*, 2782−2789.
(23) Shapiro, N. D.; Toste, F. D. *Proc. Natl. Acad. Sci.U.S.A.* **2008**, *105*, 2779−2782.
(24) Nechaev, M. S.; Rayón, V. M.; Frenking, G. *J. Phys. Chem. A* **2004**, *108*, 3134−3142.
(25) Kim, C. K.; Lee, K. A.; Kim, C. K.; Lee, B.; Lee, H. W. *Chem. Phys. Lett.* **2004**, *391*, 321−324.
(26) Hertwig, R. H.; Koch, W.; Schröder, D.; Schwarz, H.; Hrušák, J.; Schwerdtfeger, P. *J. Phys. Chem.* **1996**, *100*, 12253−12260.
(27) Ziegler, T.; Rauk, A. *Inorg. Chem.* **1979**, *18*, 1558−1565.
(28) de Haro, T.; Nevado, C. *Synthesis* **2011**, 2530.
(29) Boorman, T. C.; Larrosa, I. *Chem. Soc. Rev.* **2011**, *40*, 1910.
(30) Cheong, P. H.-Y.; Morganelli, P.; Luzung, M. R.; Houk, K. N.; Toste, F. D. *J. Am. Chem. Soc.* **2008**, *130*, 4517.

DOI: 10.1021/ct500849m
J. Chem. Theory Comput. XXXX, XXX, XXX−XXX

(31) Brown, T. J.; Widenhoefer, R. A. *Organometallics* **2011**, *30*, 6003−6009.
(32) Grirrane, A.; Garcia, H.; Corma, A.; Álvarez, E. *ACS Catal.* **2011**, *1*, 1647−1653.
(33) Simonneau, A.; Jaroschik, F.; Lesage, D.; Karanik, M.; Guillot, R.; Malacria, M.; Tabet, J.-C.; Goddard, J.-P.; Fensterbank, L.; Gandon, V.; Gimbert, Y. *Chem. Sci.* **2011**, *2*, 2417−2422.
(34) Grirrane, A.; Garcia, H.; Corma, A.; Álvarez, E. *Chem.—Eur. J.* **2013**, *19*, 12239−12244.
(35) Gómez-Suárez, A.; Nolan, S. P. *Angew. Chem., Int. Ed.* **2012**, *51*, 8156−8159.
(36) Obradorsa, C.; Echavarren, A. M. *Chem. Commun.* **2014**, *50*, 16−28.
(37) Becke, A. D. *J. Chem. Phys.* **1993**, *98*, 5648−5652.
(38) Lee, C. T.; Yang, W. T.; Parr, R. G. *Phys. Rev. B: Condens. Matter* **1988**, *37*, 785−789.
(39) Roithová, J.; Hrušak, J.; Schröder, D.; Schwarz, H. *Inorg. Chim. Acta* **2005**, *358*, 4287−4292.
(40) Nieto-Oberhuber, C.; López, S.; Jiménez-Núñez, E.; Echavarren, A. M. *Chem.—Eur. J.* **2006**, *12*, 5916−5923.
(41) Shi, F.-Q.; Li, X.; Xia, Y.; Zhang, L.; Yu, Z.-X. *J. Am. Chem. Soc.* **2007**, *129*, 15503−15512.
(42) Kovács, G.; Ujaque, G.; Lledós, A. *J. Am. Chem. Soc.* **2008**, *130*, 853−864.
(43) Mazzone, G.; Russo, N.; Sicilia, E. *Organometallics* **2012**, *31*, 3074−3080.
(44) Kang, R. H.; Chen, H.; Shaik, S.; Yao, J. *J. Chem. Theory Comput.* **2011**, *7*, 4002−4011.
(45) Nava, P.; Hagebaum-Reignier, D.; Humbel, S. *ChemPhysChem* **2012**, *13*, 2090−2096.
(46) Pašteka, L. F.; Rajskỳ, T.; Urban, M. *J. Phys. Chem. A* **2013**, *117*, 4472−4485.
(47) Rang, R. H.; Lai, W.; Yao, J.; Shaik, S.; Chen, H. *J. Chem. Theory Comput.* **2012**, *8*, 3119−3127.
(48) Faza, O.; Rodrǵuez, R.; López, C. *Theor. Chem. Acc.* **2011**, *128*, 647−661.
(49) Correa, A.; Marion, N.; Fensterbank, L.; Malacria, M.; Nolan, S.; Cavallo, L. *Angew. Chem., Int. Ed.* **2008**, *47*, 718−721.
(50) Ciancaleoni, G.; Rampino, S.; Zuccaccia, D.; Tarantelli, F.; Belanzoni, P.; Belpassi, L. *J. Chem. Theory Comput.* **2014**, *10*, 1021−1034.
(51) Frisch, M. J.; Trucks, G. W.; Schlegel, H. B.; Scuseria, G. E.; Robb, M. A.; Cheeseman, J. R.; Scalmani, G.; Barone, V.; Mennucci, B.; Petersson, G. A.; Nakatsuji, H.; Caricato, M.; Li, X.; Hratchian, H. P.; Izmaylov, A. F.; Bloini, J.; Zheng, G.; Sonnenberg, J. L.; Hada, M.; Ehara, M.; Toyota, K.; Fukuda, R.; Hasegawa, J.; Ishida, M.; Nakajima, T.; Honda, Y.; Kitao, O.; Nakai, H.; Vreven, T.; Montgomery, J. A., Jr.; Peralta, J. E.; Ogliaro, F.; Bearpark, M.; Heyd, J. J.; Brothers, E.; Kudin, K. N.; Staroverov, V. N.; Kobayashi, R.; Normand, J.; Raghavachari, K.; Rendell, A.; Burant, J. C.; Iyengar, S. S; Tomasi, J.; Cossi, M.; Rega, N.; Millam, J. M.; Klene, M.; Knox, J. E.; Cross, J. B.; Bakken, V.; Adamo, C.; Jaramillo, J.; Comperts, R.; Stratmann, R. E.; Yazyev, O.; Austin, A. J.; Cammi, R.; Pomelli, C.; Ochterski, J. W.; Martin, R. L.; Morokuma, K.; Zakrzewski, V. G.; Voth, G. A.; Salvador, P.; Dannenbuerg, J. J.; Dapprich, S.; Daniels, A. D.; Farkas, O.; Foresman, J. B.; Ortiz, J. V.; Cioslowski, J.; Fox, D. J. *Gaussian 09*, revision D.01; Gaussian, Inc.: Wallingford, CT, 2009.
(52) Grimme, S.; Antony, J.; Ehrlich, S.; Krieg, H. *J. Chem. Phys.* **2010**, *132*, 154104.
(53) Andrae, D.; Häussermann, U.; Dolg, M.; Stoll, H.; Preuss, H. *Theor. Chim. Acta* **1990**, *77*, 123−141.
(54) Fukui, K. *J. Phys. Chem.* **1970**, *74*, 4161−4163.
(55) Gonzalez, C.; Schlegel, H. B. *J. Chem. Phys.* **1989**, *90*, 2154−2161.
(56) Tomasi, J.; Mennucci, B.; Cammi, R. *Chem. Rev.* **2005**, *105*, 2999−3093.
(57) Cooper, J.; Ziegler, T. *Inorg. Chem.* **2002**, *41*, 6614−6622.
(58) Tobisch, S. *Chem.—Eur. J.* **2005**, *11*, 3113−3126.

DOI: 10.1021/ct500849m
J. Chem. Theory Comput. XXXX, XXX, XXX−XXX